Conceptual design-optimisation of a future hydrogen-powered ultrahigh bypass ratio geared turbofan engine

Swapnil S. Jagtap [a], Peter R.N. Childs [b] and Marc E.J. Stettler [a*]

[a] Department of Civil and Environmental Engineering, Imperial College London, London SW7 2AZ, United Kingdom

[b] Energy Futures Lab, Imperial College London, London SW7 2AZ, United Kingdom

* Corresponding author: m.stettler@imperial.ac.uk

Abstract

Liquid hydrogen (LH_2) is a proposed option to decarbonise long-haul aviation. LH_2 aircraft (combustion-based) is expected to be lighter than Jet-A aircraft which necessitates reduction in the engine thrust requirement. Thus, the thermodynamic and energy performance of a LH_2 aircraft engine, and its design and optimisation, is of significance. In a first, a conceptual design and optimization of a future LH_2 powered ultra-high bypass-ratio geared turbofan engine is conducted for reduced aircraft thrust requirement, using GasTurb 13 software and implementing future materials and component efficiencies. The thrust specific energy consumption (TSEC) of the optimised LH_2 engine is 6 – 8% lower than Jet-A. The TSEC of LH_2 engine is lower than Jet-A due to hydrogen's higher gravimetric energy density during combustion, higher specific heat of combustion products, and reduced thrust requirement. It is observed that optimised LH_2 engine has 11% smaller diameter, 5.5 – 7.5% shorter length, 6 – 14% lower turbine entry temperature and 7.4 – 17.6% lower weight, than a Jet-A engine. The results of this work will be useful to future studies on LH_2 engine and aircraft design, and LH_2 aircraft emissions and contrails modelling.

Keywords

Hydrogen gas turbine engine, hydrogen aircraft, alternative aviation fuel, decarbonising long-range aviation

Nomenclature

BLI	Boundary layer ingestion
BPR	Bypass ratio
BWB	Blended wing body
CMC	Ceramic matric composites
FAR	Fuel-air ratio
FPR	Fan pressure ratio
GTF	Geared turbofan
GTOW	Gross take-off weight
HPC	High pressure compressor
HPT	High pressure turbine
IPC	Intermediate pressure compressor
LH_2	Liquid hydrogen
LPT	Low pressure turbine
LTA	Large twin aisle
OPR	Overall pressure ratio
P_3	Total pressure at combustor inlet
SLS	Sea level static
SPK	Synthetic paraffin kerosene
TET	Turbine entry temperature
TOC	Top of climb
TSEC	Thrust specific energy consumption
TSFC	Thrust specific fuel consumption
T/W	Thrust to weight ratio
T_2	Fan inlet temperature

T_3	Total temperature at combustor inlet
T_4	Turbine entry temperature
UHB	Ultra-high bypass ratio
VLTA	Very large twin aisle
Φ	Equivalence ratio

1. Introduction

Aviation demand is expected to double in the next two decades (2023 – 2042) even accounting the effects of the global COVID-19 pandemic [1]. The aviation sector presently contributes to 3.5% of the total manmade radiative forcing [2,3] but the forecasted growth in aviation demand will increase its relative contribution of climate impacts. The industry predicts that the use of low-carbon fuels and advanced aircraft technology could collectively contribute to 80% of the efforts required for carbon neutral growth [4].

Presently, only blended synthetic paraffin kerosene (SPK) from different manufacturing pathways (maximum 50% blending) is approved as an alternative fuel for civil aviation use [5–9]. Liquid hydrogen (LH_2) as an aviation fuel is attractive due to its zero-carbon emissions at the point of use in an aircraft. Long-haul aviation is a challenging sector to decarbonise [10,11]. Jagtap et al. [10,11] examined and reviewed different liquid fuels, energy vectors, and different propulsion systems (including batteries and fuel cells) for long-range large aircraft application. The authors observed that LH_2 (used in combustion-based engines) and 100% SPK are the only two alternative fuels for typical long-range flight in a conventional tube-wing large twin aisle (LTA) aircraft [10], and that improving overall efficiency and aircraft aerodynamics could make LH_2 powered long-range aircraft more energy efficient compared to present-day Jet-A aircraft [12].

LH_2 as a fuel could power an aircraft via fuel cells (short-/mid- range small/mid-size aircraft) and/or combustion in gas turbine engines (large long-range aircraft) [10,13].

Different studies [14,15,24–33,16,34–43,17–23] on LH_2 aircraft focus on regional-/small-sized to mid-sized tube-wing aircraft. Other studies on long-range LTA LH_2 aircraft focus only on tube-wing aircraft performance modelling [44,45,54,55,46–53] or are not completely powered by LH_2 [56].

Jagtap et al. [10,12] observed that the gross take-off weight (GTOW) of (tube-wing) LH_2 aircraft could reduce by 20% using the present aircraft technology and by 34% using 2050 aircraft technology. Similar observations are made in studies [49,57,58]. This significant drop in the LH_2 aircraft GTOW necessitates a reduction in the engine thrust requirement [10,12,35,58–61], which would decrease the size of an LH_2 engine [59–61] and thus engine cycle design and optimisation is necessary for LH_2 use.

Considering the above discussion, the scope of the present work is limited to combustion based LH_2 engine and its cycle design, and optimisation of the engine cycle is necessary to meet the reduced thrust requirement. Fuel cells are not explored in this work. Furthermore, the literature review below is focussed only on turbofan engine cycle and performance modelling, particularly for LH_2 engine design and optimization for reduced thrust requirement and for its off-design performance. This enables LH_2 aircraft performance estimation at a conceptual design stage. The reader is advised to explore works by: Brewer [50] for LH_2 aircraft design performance, cryogenic tanks, and other aircraft subsystems design; Tiwari et al. [13] (review study) on LH_2 aircraft subsystems, combustors and fuel cell systems, and studies by Prater [62] and Marek [63] on hydrogen combustors. In terms of literature on engine modelling, there are a limited number of studies [40,64,73–81,65–72] that provide engine cycle modelling data, especially for LH_2 engines, and these are reviewed next concisely. None of these studies provide a detailed design and optimisation of a 100% hydrogen powered engine for reduced thrust requirement and these do not provide engine data on off-design performance at different points in the aircraft mission profile.

A study by Bijewitz et al. [64] designs (on-design point) an ultra-high bypass ratio (UHB) geared turbofan (GTF) engine for future aviation application using GasTurb 11 [82]. A study by Kestner et al. [65] simulates a future UHB engine to be used on a BWB aircraft (with podded engines or boundary layer ingestion) using NPSS [83]. A study by Greitzer et al. [73] designs a futuristic UHB engine using a novel and unconventional engine with four fans and two cores using NPSS [83] (for on-design) and GasTurb [82] (for off-design). A study by Nickol et al. [74] simulates the performance of futuristic UHB engines using NPSS [83]. The above studies are limited to only includes Jet-A engine performance modelling.

A study by Beck et al. [67] conducts a first order examination of a large quad or very large twin aisle (VLTA) LH_2 powered blended wing body (BWB) aircraft. However, there is no engine modelling conducted in this study and it calculates the thrust specific fuel consumption (TSFC) using a scaling factor based on the gravimetric energy density.

Studies [66,68–72,75,79–81] simulate the performance of turbofan engines powered by LH_2, and a concise review of these is conducted below followed by their shortcomings combined together as the limitations are common in all studies. Corchero et al. [66] conducts performance simulation of low bypass ratio (BPR) direct-drive turbofan engine powered by LH_2 using GasTurb 8 [82]. Verstraete [81] simulates the performance of a low BPR LH_2 engine in GasTurb 12. Atma et al. [68] calculates the performance of a futuristic LH_2 powered UHB engine using NPSS [83]. Osigwe et al. [69] simulates a low BPR direct-drive turbofan engine powered by LH_2 using their in-house developed model. Balli et al. [72] estimates the performance of a TF33 (low BPR) LH_2 powered engine using their in-house model. Additionally, studies by Boggia et al. [79] and Jackson [80] model low BPR turbofan engine powered by LH_2 using GasTurb 3.8. A study by Carter et al. [70] conducts performance simulation of a futuristic LH_2 powered high BPR engine using NPSS [83]. A study by Görtz et al. [71] models the performance of a futuristic LH_2 powered UHB engine using GTlab [84] at cruise. As previously discussed, hydrogen aircraft are expected to have significantly lower GTOW than Jet-A. Therefore, the thrust requirement would be lower, and engine has to be optimized according to this reduced thrust requirement, thereby decreasing the size of engine. All of the above studies [66,68–72,75,79–81] simulate (uninstalled) engine performance of an unoptimized hydrogen engine for same turbine entry temperature (TET) (or higher thrust) and/or same thrust production (or lower TET) as that of Jet-A, and the engine performance data at off-design points are missing.

A study by Marszalek [75] conducts performance simulation of an unoptimized low BPR turbofan engine powered by LH_2 in MATLAB. However, it simulates (uninstalled) engine performance for a thrust value which is greater than that of Jet-A (rationale for this choice is unknown). A study by Emine et al. [77] simulates the performance of hydrogen in GEnx high bypass turbofan engine in 'engineering equation solver' software. However, the baseline engine performance is unknown and thus performance comparison of hydrogen and Jet-A engine cannot be conducted.

A study by Nercy et al. [58] models LH_2 aircraft performance using simple engine performance estimation (in MATLAB) and this is disclosed in a study by Palies [78]. The engine performance calculation by Palies [78] is done for using a isentropic thermodynamics-based model for a thermal-powered narrow-body aircraft hydrogen-based engine. ~~The engine performance estimation by Palies [78] is done using a simple isentropic thermodynamics-based model.~~ In the study by Nercy et al. [58], ~~though~~ the author mentions that reduced aircraft mass implies reduced thrust resulting in reducing fuel flow rate.~~,~~ The engine performance modelling is described in the studies by Palies [78] whereas the effect of fuel weight is discussed in Nercy et al. [58]. ~~the details of engine performance modelling is not disclosed in the studies by Nercy et al. [58] and Palies [78].~~ Additionally, the latter study includes limited engine cycle data at cruise and sea level static (SLS), and other off-design points are missing. ~~It is unclear from the study by Palies [78] due to limited data disclosed, which is the on-design point and how the off-design point performance is estimated.~~ For LH_2 engine, the emissions, fuel flow rate, and adiabatic flame temperatures are known at cruise and take-off. In Palies [78], the hydrogen engine operates at same thrust between baseline engine fuelled by sustainable aviation fuel (SAF) and LH_2. The engine cycle performance model with all equations is described in Palies [78]. The prior work [78] established a retrofitting procedure for hydrogen aircraft and the present work builds upon it by considering the effect of reduced aircraft weight on reduced thrust requirement and all major off-design points with on-design point analysis, for a clean-sheet (non-retrofit) design. ~~For LH_2 engine, the emissions, fuel flow rate, and adiabatic flame temperatures are known at cruise and SLS. However, it is unclear whether the hydrogen engine operates at same thrust or modified thrust compared to their baseline engine fuelled by sustainable aviation fuel (SAF). The engine cycle performance data at all aircraft flight mission points are unknown from studies by Nercy et al. [58] and Palies [78]. Overall, the data disclosed in these studies are unclear and insufficient to be replicated or to be used for estimating engine/aircraft performance at on-design and all off-design points. However, they have substantial data on detailed design of different combustor technologies and resulting emissions, which is out of the scope of this work.~~

A study by Derakhshandeh et al. [76] model the (uninstalled engine) design point performance of hydrogen powered General Electric GE90 turbofan engine cases (unoptimized and optimized) in MATLAB. The baseline engine BPR, overall pressure ratio (OPR), TET, and thrust are 8.1, 40.4, 1380.7 K, and 72.45 kN, respectively. For the unoptimized hydrogen engine only TET and thrust are known to be 1487.52 K and 80.59 kN, respectively. Lastly, for the optimized hydrogen engine, the BPR, OPR, TET, and thrust are 10.3, 39.49, 1487.52 K, and 84.24 kN, respectively. It can be observed that the design characteristics of the unoptimized and optimized hydrogen engines are completely different than the baseline (GE90 turbofan engine). The rationale for this is not explained by Derakhshandeh et al. Therefore, any direct comparison of engine performance due to the use of hydrogen relative to Jet-A cannot be made.

In summary, it can be observed from above reviewed studies [58,66,78–81,68–72,75–77] on hydrogen engine cycle performance that there is clearly a need for a more detailed design and optimisation of a 100% LH_2 powered engine and its performance at off-design points, to meet the reduced thrust requirement of an LH_2 aircraft, and this is missing from the existing literature and thus motivates the present work.

The objective of this work is to model the performance metrics of a future UHB GTF using Jet-A and LH_2 (separately) at on-design and off-design points, where the LH_2 engine is optimized for reduced thrust requirement. Using the engine on-design and different off-design points data for Jet-A and LH_2 (separately), the aircraft performance can be accurately predicted as compared to using the simple Breguet range equation analysis conducted previously in [10,12,58]. Studies on the above discussed aspects are missing from literature and thus are novel contributions of this work. The above analysis will be conducted using a conceptual engine design process. The findings from this research will benefit future studies on design of LH_2 engine and aircraft, as well as the modelling of LH_2 aircraft emissions and contrails. To contextualise this work, a review of aircraft and engine design process is included in Supplementary Information (SI) §1.1 and a review of the conceptual engine design process is included in SI §1.2. The methodology for engine design is detailed in §2 followed by results and discussion in §3. The engine performance estimation in this work is a low fidelity analysis and errors in engine performance metrics are expected. More limitations of this research are included in §3.3. Details excluded from the main body are included in the SI document.

2. Methodology

In this work, UHB GTF engines powered by Jet-A and LH_2 (separately) are modelled for a futuristic blended wing body (BWB) aircraft seating 301 passengers. This aircraft configuration is selected because a significant amount of information on the baseline (Jet-A) engine and aircraft design for conducting a conceptual design study is available from NASA's studies [74,85–87]. In this work, design and optimisation of the UHB GTF engine is conducted using commercial software called GasTurb 13 [88] and conceptual engine design approach from literature (reviewed in SI §1.2). An overview of GasTurb 13 software is provided in SI §1.4 with details of optimisation algorithm that searches for the global optimum.

2.1 Design cases

Table 1. Different engine design cases explored in this work

Case	Description
Baseline (Jet-A)	UHB GTF engine powered by Jet-A (20% cooling flows)
LH_2 case 1	UHB GTF engine powered by LH_2, and the thrust production is same as that of the baseline Jet-A engine (20% cooling flows)
LH_2 case 2	UHB GTF engine powered by LH_2, and the engine is optimized for reduced thrust requirement and it is smaller in size (20% cooling flows)
LH_2 case 3	UHB GTF engine powered by LH_2, and the engine is optimized for reduced thrust requirement and it is smaller in size (no cooling flows)

Table 1 lists the different engine design cases explored in this work and the rationale behind these cases is detailed next. The UHB GTF design cases that will be considered in this work are: the baseline case (Jet-A) with 20% cooling flows, and three cases of LH_2 fuel; where the engines use advanced materials for withstanding higher temperatures compared to the present-day engines. The overview of conditions in the three cases of LH_2 fuel analysed are as follows:

- Case 1 is where the aircraft thrust production remains the same as that of Jet-A case, and typical (20%) engine cooling flows are employed.
- LH_2 fuel is more energy dense than Jet-A, and thus less mass of LH_2 fuel is required at the start of the mission. Therefore, for similar thrust to weight ratio (*T/W*) as that of the baseline aircraft, the thrust requirement decreases. Dincer [59], Verstraete [60], and Nojoumi [61] support that for an LH_2 powered aircraft, the thrust requirement reduces and the engine becomes smaller in size. Case 2 is where the aircraft thrust requirement and engine size reduces for maintaining similar *T/W* as that of Jet-A case, with typical (20%) engine cooling flows.
- Corchero et al. [66] and Verstraete [60,81] find that the TET in a hydrogen powered gas turbine engine is lower than Jet-A engine for same engine thrust production. Case 3 is Case 2 without engine cooling flows, since the engine TET is expected to be lower than the baseline case because of reduced thrust requirement, where the engine uses advanced materials for withstanding high temperatures in baseline case (Jet-A), Case 1 and Case 2.

2.2 Model description

The engine design requirements are listed in Table 2. Further details about the engine and aircraft are included in SI §2.1 and SI §2.2. The engine design requirements in Table 2 remain the same for Jet-A and LH_2 Case 1. For LH_2 Case 2 and Case 3, the 'engine diameter' constraint is removed as suggested by Dincer [59], Verstraete [60], and Nojoumi [61]. It is to be noted that the OPR, BPR, and FPR for all hydrogen engine cases are same as that of Jet-A engine and this is consistent with the considerations made in studies [66,79–81]. This is because these are basic design requirements and in this study (only) the impacts of fuel switch on engine design and performance is being examined.

Table 2. Engine design requirements

Parameters	Units	Top of climb (TOC)	Sea level static (SLS)

Mach and altitude	- , m	0.8 at 10,668 m	0, 0 m
Net thrust	kN	55.603	299.9
Overall pressure ratio (OPR)	-	60.0	47.1
BPR	-	17.65	20
Fan pressure ratio (FPR)	-	1.35	1.25
Fan diameter*		132.4 inches or 3.36296 m	
Power off-take	kW	150	
Bleed	-	Zero	
Drive and engine type	-	Geared turbofan engine	
* is a design requirement only for baseline (BWB Jet-A) case and LH_2 case 1			

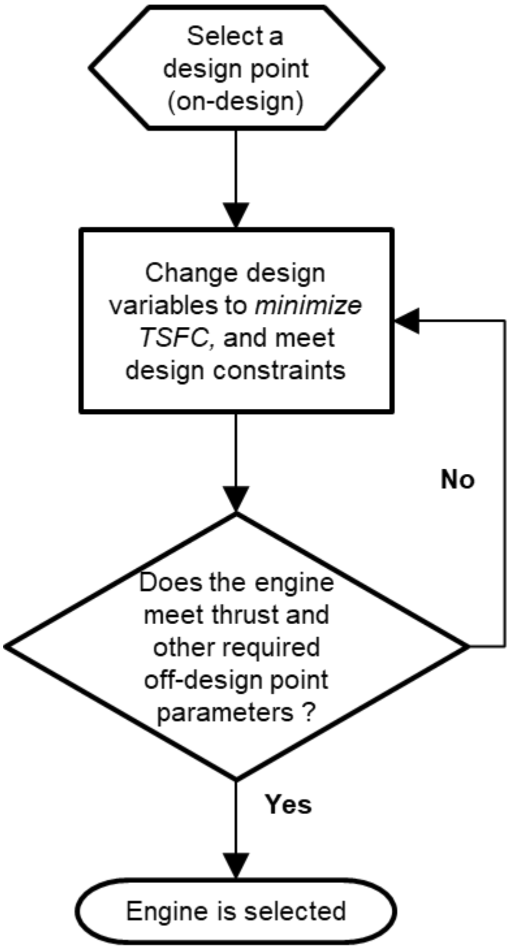

On-design point:

Variables:
- Gearing ratio
- Mass flow rate (inlet standard corrected flow)
- Turbine entry temperature (T_4)
- Pressure ratios: Fan, Intermediate pressure compressor (IPC), High pressure compressor (HPC)
- Tip speed: Fan tip speed, HPC

Constraints:
- Required thrust
- Bypass ratio (BPR)
- Fan pressure ratio (FPR) and overall pressure ratio (OPR)
- Power off-take
- Satisfactory aerodynamic performance of turbomachinery and mechanical design of their disks
- Fan diameter (except LH_2 case 3)
- 20% Cooling flows (except LH_2 case 3)

Off-design point:

Variables:
- Efficiencies of fan, IPC, and HPC
- Fan capacity
- Bypass pressure

Constraints:
- Required thrust (if known)
- BPR, OPR, and FPR (if known)
- Satisfactory aerodynamic performance of turbomachinery and mechanical design of their disks
- 20% Cooling flows (except LH_2 case 3)

Figure 1. Engine design-optimisation schematic used in this work

After reviewing conceptual engine design process (in SI §1.2), a simple schematic focussed only on the engine design and optimisation process (not explicitly stating the aircraft drag polar here) is created as shown in Figure 1. This is based on the schematic of Walsh and Fletcher [89,90] (see Figure SI 4 in SI §1.2). The engine design point is called as the 'on-design' operational point. Once the engine is designed (fixed engine), its performance is tested at other operational points in aircraft mission, and these are called as 'off-design' points (discussed in §2.5).

Referring to Figure 1, the design and optimisation process starts with the selection of the design point (on-design). The top of climb (TOC) condition is the on-design point because maximum engine inlet corrected flow is at this point [64]. There are inputs in the engine model such as engine/component design parameters, component efficiencies, turbine cooling flows, materials (conventional and advanced), component stage counts, and combustor technology. These are detailed in SI §2.3.

After the engine model is ready with these inputs, design variables for the optimisation process are identified. There is an initial guess value assigned to each of the design variables for initiating the optimisation process. For example: TET or T_4 is set as a design variable and at the design point its value is unknown. A realistic value of 1,750 K is input to the model as a starting guess. Ceramic matric composites (CMC) are used for the hot end components, and thus a maximum value of 2,173 K (based on literature) is provided to the design variable (see discussion in SI §2.3.3).

After selecting the design variables, the design constraints are identified. For example: thrust is one of the constraints in the design-optimisation process, where minimum required value must be met for the aircraft to fly. For the baseline case using conventional jet fuel, at the TOC condition it is necessary to produce at least the thrust value as per the design requirements listed in Table 2 (of 55.603 kN). The figure of merit or the objective of the optimisation process is to minimise the thrust specific fuel consumption (TSFC [g/kN.s], which is the ratio of fuel consumption rate to the thrust). During the optimisation process in

GasTurb 13, the design variables are perturbed within their set limits such that the specified design constraints are met for minimising the TSFC. Once this process is finished, the turbomachinery of this engine configuration is checked for a satisfactory aerodynamic performance of individual turbomachinery stages (aerodynamic and geometrical factors) using standard/GasTurb 13 default turbomachinery inputs (degree of reaction, flow coefficient, and stage loading). Once a satisfactory aerodynamic performance of the turbomachinery is obtained, the engine performance at different off-design points is evaluated using GasTurb 13. Only if the engine meets the off-design parameters including the thrust requirements, the engine is selected as a final candidate. It is to be noted that the point-to-point axial location of the engine is available in GasTurb 13, and the length and diameter of different components can be easily estimated. The combustor exit (axial) gas velocity and length of the 'combustor can' (in §3.1) is estimated from the point-to-point axial locations known from GasTurb 13.

The design-optimisation parameters are discussed next. The model inputs are detailed in SI §3.2. Some of these inputs change between baseline case, and the three cases of LH_2 fuel, and the changes are identified/reported accordingly in SI §3.2.

2.3 Design-optimisation parameters

Table 3. Design variables in the engine design-optimisation process

Variable		Units	Minimum value	Starting guess value	Maximum value
Gearing ratio		-	2.5:1	3:1 [91]	4.5:1 [64]
Mass flow rate (inlet standard corrected flow)		kg/s	1,400 [92]	1,700	1,800
TET (T_4)		Kelvin (K)	1,400	1,750 [64]	2,173 [93]
FPR	Inner	-	1.1	1.33	1.35 [74]
	Outer		1.1	1.34	1.35 [74]
IPC pressure ratio [92]		-	1.1	3	10
HPC pressure ratio [65]		-	1.1	15	25
Fan tip speed		m/s	300	380	411.48 [92]
HPC tip speed		m/s	250	360	382.84 [92]

IPC: Intermediate pressure compressor, HPC: High pressure compressor

The known data on engine technology and components is discussed in SI §2.3. However, some engine design data (or approximate values) such as the pressure ratio of the compressors, gearing ratio, TET, tip speeds of fan and high-pressure compressor, and engine inlet mass flow rate, are unknown. These parameters can be estimated using the optimisation process. The design variables considered in this work, are as listed in Table 3. Referring to Table 3, the design variables and their extreme values are based on prior studies. The detailed rationale for the range of the design variables is included in SI §3.1.

2.4 Disk optimisation and engine weight

The finalised engine model is then checked for shape and stress in all disks, and at all points in the flight envelope considered in this work. An ‘I-section’ for the disk’s shape is selected owing to its resistance to bending and shear forces acting on it [94]. The disk optimisation is done in GasTurb 13, where the software flags overstressed disks. At the design point, the disk shape and stress for each stage of each turbomachine is analysed for satisfactory mechanical performance and minimisation of weight. After this is fulfilled, the mechanical performance of each disk of all turbomachines is analysed at all off-design points considered in this work. If some disks remain overstressed at some off-design points, then those disks must be redesigned at the on-design point and later checked for their off-design point mechanical performance. This process is iterated until all disks have satisfactory mechanical performance at on-design point and all off-design points considered in this work.

The engine materials data are input into the model at the beginning of the on-design analysis. Once the disk design-optimisation is completed, the engine weight is calculated. This is the bare engine weight without accessories (like control unit), engine mount, and nacelle. The bare engine weight includes the engine’s principal components (included in SI

§2.3.3 in Table SI 9 and Table SI 10), and supplementary components such as nuts, bolts, washers, seals, piping, and pumps. The weight of the principal engine components is estimated from the material densities (from SI §2.3.3) input into GasTurb 13. The weight of the above-mentioned supplementary components is estimated by using a mass-factor (multiplication factor) to the principal engine weight. Halliwell [95] uses a mass factor of 1.2 and GasTurb 13's default mass factor value is 1.3. An average mass factor value of 1.25 is used in this model to estimate the bare engine weight. The bare engine weight, and TSFCs at on-design point and different off-design points, are estimated using the above process. The summation of weights of nacelle, accessories, and engine-mount, with the engine bare weight equals the total engine pod weight. The weights of nacelle, accessories, and engine-mount are not calculated separately, and are used as is from literature and these are listed in Table SI 2 (SI §2.1).

The engine weight and TSFCs obtained from the above engine model at on-design point and different off-design points are input to the BWB aircraft weight sizing (described in resource [96]). This in-turn determines the thrust requirements at various points in the BWB aircraft mission. The aircraft design is an iterative and interactive process, and it continues until the thrust value evaluated after the aircraft weight sizing process converges with the thrust produced by the engine in the present iteration of engine design-optimisation. In this work, only the calculated thrust values (from resource [96]) for engine design are included for the multiple cases discussed here.

2.5 Off-design analysis

All inputs for on- and off-design analysis have been listed and discussed so far. The on-design analysis can be conducted using the above discussed inputs and process. The off-design analysis is conducted with the help of maps, which is a standard procedure. In the current work, this is done in GasTurb 13 software. 'Standard maps' are selected in GasTurb

13 for climb, cruise, and loiter points, for conducting off-design analysis at these points. The data of ambient conditions at these points from Table SI 13 (in SI §3.2), are input to the model. A feature in GasTurb 13 of off-design modifiers through iteration of parameters, is used for the turbomachinery parameters such that every turbomachine operates at the efficiencies listed in Table SI 6 (in SI §2.3.1) at respective points of climb, cruise, and loiter. The identified iteration parameters and their target parameters are listed in Table 4, along with the respective design requirements met. For loiter, there is no separate column of component efficiencies. In this work, loiter is treated as additional cruise stage and therefore efficiencies of the cruise point are selected. Thus, every turbomachine operates at its respective efficiency during climb, cruise, and loiter. It is to be noted that for all off-design points except SLS, the target component efficiencies are known, and BPR, OPR, and FPR are unknown from Table 2 (and Table SI 1 – Table SI 4 in SI §2), and thus only the target component efficiencies at these points are set as a design requirement. Therefore, the 'design parameter' section of Table 4 is not used in the off-design iteration for climb, cruise, and loiter.

SLS is a special off-design point in this work where not only turbomachinery efficiencies but also the performance/design requirements are to be met (see Table 2). For SLS condition, the option of 'selected map' is chosen in GasTurb 13. After choosing it, map option for a single-stage fan, sub-sonic IPC/booster, 'high pressure ratio' for HPC, 'two-stage' high pressure turbine (HPT), and 'medium pressure ratio' low-pressure turbine (LPT) is selected in GasTurb 13. Similar to the above discussed process, the off-design modifiers feature is used through iteration of parameters. In GasTurb 13, off-design case is employed such that the target SLS turbomachinery efficiencies listed in Table SI 6 (in SI §2.3.1) and all performance/design requirements at SLS, are met.

To validate the model, two engine cases from literature are considered and the respective engine designs (with case specific design targets) are successfully replicated within ±5% which is considered acceptable in the conceptual design phase [97,98]) in SI §4. These establish a confidence in the engine model. The designs for different fuel cases are developed and analysed in the next section.

Table 4. Off-design modifiers: iteration and target parameters

Iteration parameter	Target parameter	Design requirement is met for:
	Component efficiencies	
Change in efficiency of:	Efficiency of:	Efficiency of:
Δ outer LPC (fan)	outer LPC (fan)	LPC (fan)
Δ inner LPC (fan)	inner LPC (fan)	
Δ IPC	IPC	IPC
Δ HPC	HPC	HPC
Δ HPT	HPT	HPT
Δ LPT	LPT	LPT
	Design parameters	
HPC spool speed	OPR	OPR
Δ LPC capacity	Outer fan exit pressure	FPR
Δ Bypass pressure	BPR	BPR

3. Results and discussion

In this section, the results of the engine model for the set research objectives and design requirements are considered for different fuel cases. The results comprise performance analysis at on-design point and off-design points. It is to be noted that data points in Figures 1 to 3 for Case 2 of LH_2 are not included to avoid confusion as some points overlap with Case 1 points. The on- and off-design performance of the baseline (Jet-A) engine and its comparison with other engine designs in literature is detailed in SI §5.1. Similarly, for 100% SPK (similar properties as that of Jet-A) the on- and off-design performance is included in SI §5.2.

3.1 LH_2 engine design cases

Tables 5, 6, and 7 list the comparison of engine performance using Jet-A and LH_2 (three cases), at TOC (on-design), SLS, and cruise, respectively. It is to be noted that these results are for one engine. The engine performance comparison for these two fuels at other points is provided in SI §5.3 (Tables SI 34 [climb] and SI 35 [loiter]). It can be observed from

Tables 5 and 6 that the engine designs successfully meet the design requirements/targets as set in Table 2.

Table 5. Comparison of engine performance at TOC condition using LH_2 fuel (three cases) and Jet-A, using the proposed model

TOC parameters	Units	Jet-A	LH_2		
			Case 1	Case 2	Case 3
Mach, altitude	- , m	0.8 at 10,668 m	0.8 at 10,668 m	0.8 at 10,668 m	0.8 at 10,668 m
Engine mass flow	kg/s	638.1	638.1	571.9	558.8
Thrust required	kN	55.60	46.29	46.02	45.66
Thrust produced	kN	55.60	55.60	46.35	46.12
TSFC	g/kN-s	12.4	4.3	4.3	4.2
TSEC	kJ/kN-s	535.7	519.4	514.1	499.1
TSEC % difference compared to Jet-A	%	-	-3.04	-4.03	-6.82
Fuel consumption	g/s	689	241	199	192
Fuel-air ratio (FAR)	-	25.19×10^{-3}	8.79×10^{-3}	8.09×10^{-3}	6.40×10^{-3}
Equivalence ratio (Φ)	-	0.37	0.30	0.28	0.22
OPR	-	60	60	60	60
BPR	-	17.65	17.65	17.65	17.65
FPR	-	1.35	1.35	1.35	1.35
IPC pressure ratio	-	3.3	3.3	3.3	3.3
HPC pressure ratio	-	13.9	13.9	13.9	13.9
Cooling flow	%	20	20	20	Zero
Combustor can length	mm	198.1	198.1	187.2	185.1
Combustor exit gas velocity	m/s	235.7	238.5	234.3	223.6
Residence time	µs	841	831	800	826
P_3	kPa	2,159.4	2,159.4	2,159.4	2,159.4
T_3	K	859.4	859.5	859.5	859.5
T_4	K	1,689.6	1,642.4	1,588.5	1,452.5
T_4/T_2	-	6.844	6.653	6.434	5.883
Bare engine weight	kg	4,411	4,381	4,084	3,636
Gear ratio	-	3.5	3.5	3.1	3.1
Fan diameter	mm	3,362.9	3,362.9	3,183.9	3,147.1
LPT inlet temperature	K	1,139	1,111	1,060	1,054
Power off-take	kW	150			

P_3: Total pressure at combustor inlet, T_3: Total temperature at combustor inlet

Table 6. Comparison of engine performance at SLS condition using LH_2 fuel (three cases) and Jet-A, using the proposed model

SLS parameters	Units	Jet-A	LH_2		
			Case 1	Case 2	Case 3
Mach, altitude	- , m	0 at 0 m	0 at 0 m	0 at 0 m	0 at 0 m
Engine mass flow	kg/s	1,526.9	1,528.7	1,356.6	1,331.9
Thrust required	kN	299.9	251.1	249.6	247.7
Thrust produced	kN	303.9	304.5	263.8	261.1
TSFC	g/kN-s	5.12	1.78	1.76	1.69
TSEC	kJ/kN-s	221.4	213.3	211.3	202.8
TSEC % difference compared to Jet-A	%	-	-3.6	-4.5	-8.4
Fuel consumption	g/s	1557	541	465	441
FAR	-	26.91×10^{-3}	9.35×10^{-3}	9.04×10^{-3}	6.99×10^{-3}
Φ	-	0.39	0.32	0.31	0.24
OPR	-	47.1	47.1	47.1	47.1
BPR	-	20	20	20	20
FPR	-	1.25	1.25	1.25	1.25
IPC pressure ratio	-	3.03	3.04	2.89	2.95
HPC pressure ratio	-	12.77	12.70	13.39	13.03
Cooling flow	%	20	20	20	Zero
Combustor can length	mm	198.1	198.1	187.2	185.1
Combustor exit gas velocity	m/s	241.8	244.6	243.2	230.8
Residence time	µs	820	810	770	800
P_3	kPa	4,724.8	4,724.5	4,724.7	4,724.7
T_3	K	914	914	914	912
T_4	K	1,776	1,720	1,698	1,539
T_4/T_2	-	6.163	5.97	5.892	5.342
LPT inlet temperature	K	1,213	1,179	1,152	1,135
Power off-take	kW	150			

In Tables 5, 6, and 7, the engine designs meet the required thrust values for all three cases of LH_2 fuelled engine, at said mission points considered in respective tables. The values of thrust required mentioned in Tables 5, 6, and 7, are calculated through aircraft weight sizing process detailed in [96]. The LH_2 aircraft weight at different points in flight mission is lower than the Jet-A aircraft [10,12,50,96,99]. To maintain a similar *T/W*, the thrust requirement reduces for LH_2 aircraft compared to Jet-A. To account these impacts of LH_2 use in aircraft, three different cases are considered as discussed in §2.1. The engine performance in Tables 5, 6, and 7 are further discussed in §3.1.1 - §3.1.3.

Table 7. Comparison of engine performance at cruise condition using LH_2 fuel (three cases) and Jet-A, using the proposed model

Cruise parameters	Units	Jet-A	LH_2		
			Case 1	Case 2	Case 3
Mach, altitude	- , m	0.84 at 10,668 m	0.84 at 10,668 m	0.84 at 10,668 m	0.84 at 10,668 m
Engine mass flow	kg/s	649.7	649.8	602.9	569.7
Thrust required	kN	42.25	40.24	40.15	40.02
Thrust produced	kN	51.61	51.68	51.09	43.12
TSFC	g/kN-s	12.67	4.42	4.35	4.28
TSEC	kJ/kN-s	547.2	530.9	522.1	513.4
TSEC % difference compared to Jet-A	%	-	-2.98	-4.59	-6.16
Fuel consumption	g/s	654	229	222	185
FAR	-	24.10×10^{-3}	8.42×10^{-3}	7.91×10^{-3}	6.06×10^{-3}
Φ	-	0.35	0.29	0.27	0.21
Propulsive efficiency	-	0.86	0.86	0.86	0.87
Core efficiency	-	0.61	0.63	0.63	0.64
Overall efficiency	-	0.46	0.47	0.48	0.49
Transmission efficiency	-	0.87	0.87	0.88	0.87
Combustor can length	mm	198.1	198.1	187.2	185.1
Combustor exit gas velocity	m/s	231.9	234.7	234.0	219.9
Residence time	µs	854	842	801	842
P_3	kPa	2,108.3	2,110.4	2,473.6	2,162.5
T_3	K	838	838	876	843
T_4	K	1,640	1,597	1,588	1,410
T_4/T_2	-	6.567	6.394	6.359	5.645
Cooling flow	%	20	20	20	Zero
LPT inlet temperature	K	1,107	1,081	1,066	1,025
Power off-take	kW	150			

3.1.1 Effect on TET (T_4) and FAR

Table 8 lists different studies on LH_2 engine TET (T_4) reduction compared to Jet-A engine for same thrust production. It can be observed that for SLS and cruise, for same thrust production, the (%) reduction in TET (T_4) observed in this study is very similar to the findings of studies by Corchero et al. [66], Jackson [80], and Verstraete [81].

According to Corchero et al. [66], a 37 K drop in TET (T_4) increases the engine life and doubling the turbine life. Tables 5, 6, and 7 show that TET (T_4) drops by 40 – 50 K between Jet-A and LH_2 case 1, and it drops by 230 – 237 K between Jet-A and LH_2 case 3. This implies that life of LH_2 engine and turbine can be significantly improved.

Table 8. Different studies on LH_2 engine TET (T_4) reduction compared to Jet-A engine for same thrust production

	SLS TET (T_4) in Kelvin			Cruise TET (T_4) in Kelvin		
	Jet-A	LH_2	% reduction	Jet-A	LH_2	% reduction
This study (LH_2 case 1)	1,776.0	1,720.0	3.2	1,640.0	1,597.0	2.6
Corchero et al. [66]	1,507.9	1,470.9	2.5	1,103.7	1,089.5	1.3
Jackson [80]	1,472.0	1,438.0	2.3	1,288.0	1,264.0	1.9
Verstraete [81]	1,794.5	1,735.5	3.3	-	-	-

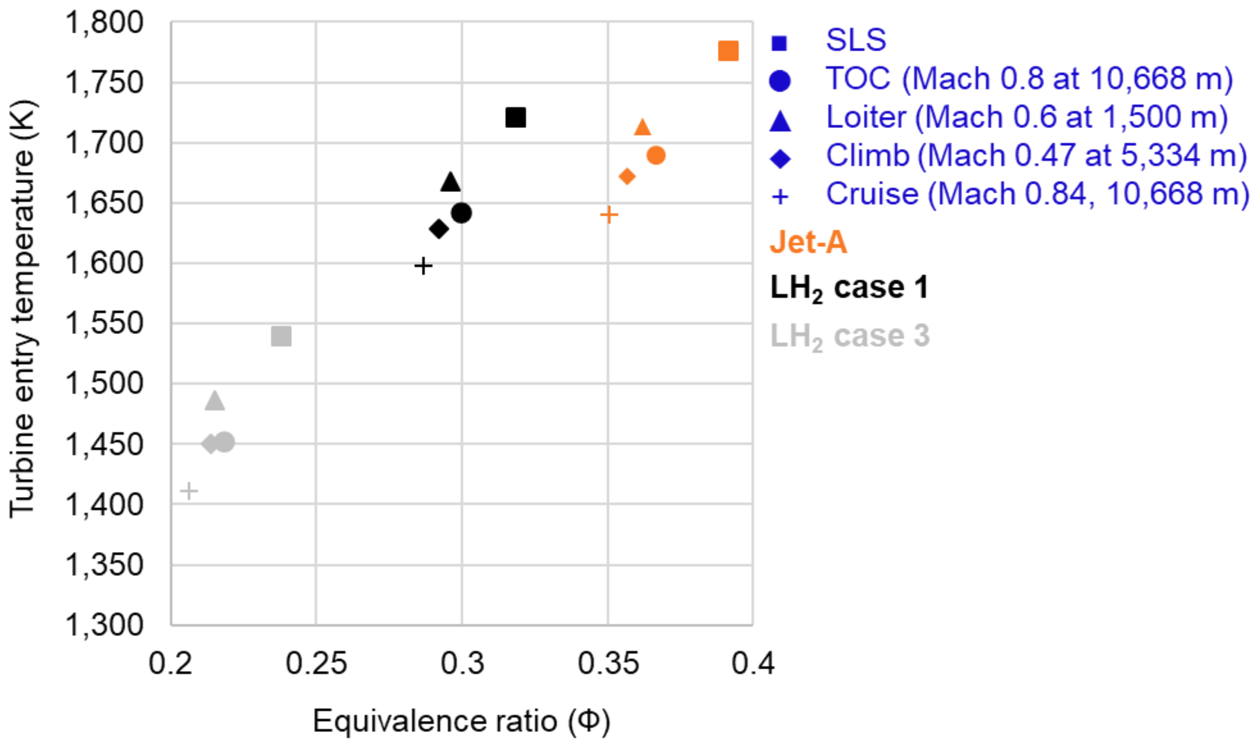

Figure 2. Turbine entry temperature and equivalence ratio (Φ) at different mission point for all fuel cases

Figure 2 summarises the TET and equivalence ratio (Φ) at different mission points for all fuel cases considered in this work. Overall, it is observed that hydrogen engines have a lower TET (T_4) and operate at lower Φ compared to Jet-A engine, at all mission points considered in this work. The reasoning behind observations made from Table 8 and Figure 2 are discussed next.

The reason for reduction in T_4 in hydrogen engines compared to Jet-A engine for same thrust production is fundamentally because of the difference in the mass and species conservation (hydrogen vs Jet-A combustion process), resulting in higher specific heat for hydrogen combustion products compared to Jet-A. It is observed that the global Φ for hydrogen is lower than Jet-A, for same thrust production at all mission points, and the local Φ comparisons need high fidelity modelling. For example, it can be observed from Table 5 and Figure 2 that at TOC, hydrogen (Case 1 [same thrust production], Φ = 0.3, and specific heat capacity at combustor exit is 1343 J/kg-k [from GasTurb 13]) has lower global equivalence ratio compared to Jet-A (Φ = 0.37 and specific heat capacity at combustor exit is 1287 J/kg-k [from GasTurb 13]). This is discussed further quantitatively and qualitatively (in SI §5.3) with the help of a simple (textbook) 'major species' combustion model (details of model in SI §1.3.1), and conservation of mass, energy, and momentum at burner exit (or at turbine entry). Additionally, a statistical mechanics approach is used (in SI §5.3, with mass, momentum, and energy conservation) to explain the difference in specific heat of combustion products of hydrogen vs Jet-A, for same thrust production. The studies by Verstraete [60,81] support that the drop in T_4 is due to an increase in the specific heat of combustion products in hydrogen engines compared to Jet-A engine, for same thrust production. Furthermore, the 'major species' combustion model is validated by predicting the emissions index (EI) of H_2O for Jet-A and LH_2 and its comparison with literature is included in SI §1.3.1.

Additionally, Figure 2 is useful to the reader for mapping out TET (T_4) and Φ for both Jet-A and LH_2 cases at on-design and different off-design points in the flight mission. Future studies could use the data from this figure to develop an equation or surrogate model that calculates TET (T_4) from the throttle setting for LH_2 engines. This would be useful for a multi-point design and optimization of LH_2 aircraft within the design space.

3.1.2 Effect on TSEC and thrust

The TSFC in Tables 5, 6, and 7 (and Tables SI 34 [climb] and SI 35 [loiter] in SI §5.3) is converted to thrust specific energy consumption (TSEC) by multiplying every case with the energy density of the respective fuel considered. Figure 3 summarises the TSEC and thrust produced at different mission point for all fuel cases. Case 3 hydrogen engine produces less thrust due to lower thrust requirement compared to Jet-A aircraft at different mission points (based on design problems set in §2.1). Overall, it is observed that all hydrogen engine cases have lower TSEC compared to Jet-A at all mission points.

It is observed that the ratio of TSFCs of Jet-A to LH_2 Case 1 (same thrust production) is 2.87, at all points in the mission, whereas the ratio of energy densities per unit mass of LH_2 to Jet-A is 2.78. For same thrust production, Verstraete [60] observes a similar ratio of TSFCs of Jet-A to LH_2 of 2.86. There are two contributing factors to this TSFC ratio. These are: 2.78 times greater gravimetric energy density of LH_2 compared to Jet-A (primary contributor); and difference in mass and species conservation of combustion of the two fuels leading to higher specific heat capacity of combustion products of LH_2 compared to Jet-A (discussed in §3.1.1). As observed from Tables 5, 6, and 7 (and Tables SI 34 [climb] and SI 35 [loiter] in SI §5.3) and Figure 3, compared to Jet-A engine, case 1 of hydrogen engine has ~3% lower TSEC, and the study by Verstraete [60] observes a similar reduction in TSEC (for same thrust production).

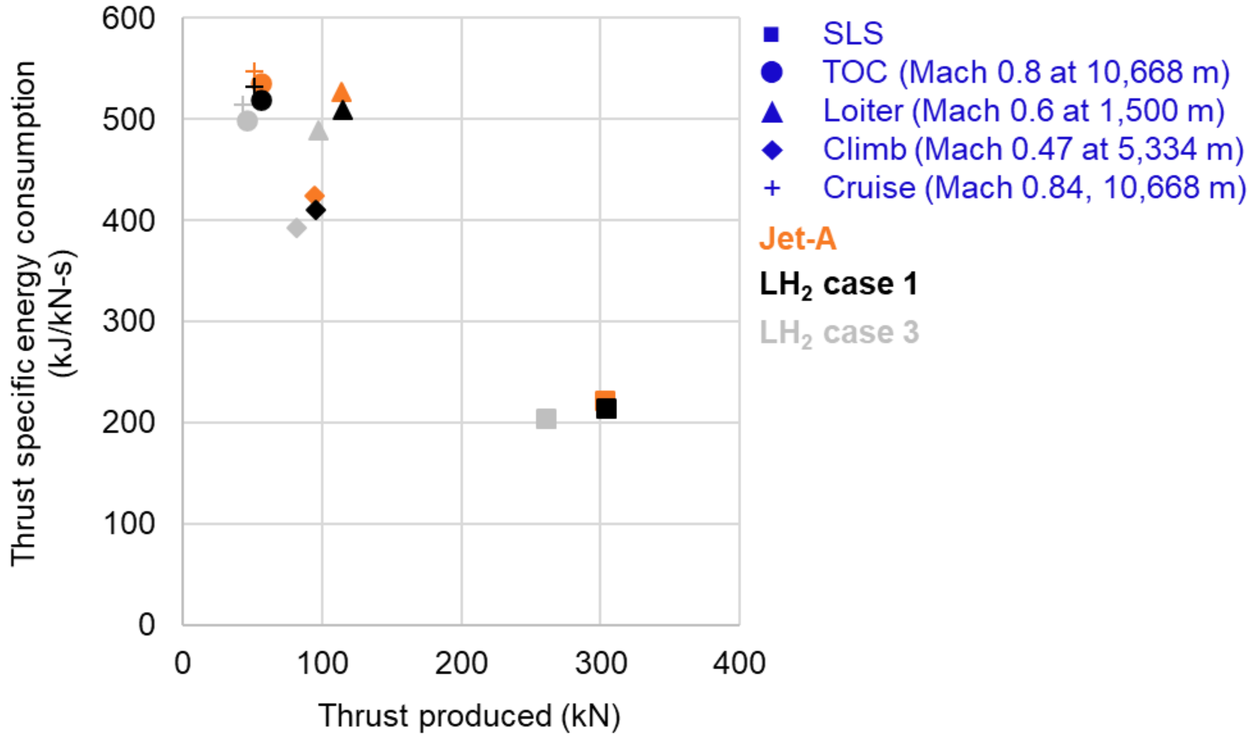

Figure 3. Thrust specific energy consumption and thrust produced at different mission point for all fuel cases

Additionally, it is known from Figure 2 that all three cases of LH_2 engine operate at a lower T_4 and Φ compared to the Jet-A engine. Additionally, it can be observed from Tables 5, 6, and 7 (and Tables SI 34 [climb] and SI 35 [loiter] in SI §5.3), that the thrust values drop between Case 1 and Case 3 of LH_2, because the effect of lighter LH_2 aircraft weight is considered. Therefore, T_4 and Φ drops between Case 1 and Case 3 of LH_2 (observed in Figure 2), which is expected. In Case 3 of LH_2, there are no cooling flows because the engine is operating at a significantly lower T_4 (approximately 200 K reduction) and the design decision (§2.1) to consider this case specifically in this work, is well supported. Because there are no cooling flows, the engine consumes less fuel compared to Case 2 of LH_2. The drop in T_4 values as discussed above along with the effect of zero cooling flows in Case 3 of LH_2, both are attributable to the (thrust or) TSFC drop between Case 1 and Case 3 of LH_2. Overall, these above discussed effects (lower T_4 and Φ, lighter aircraft or thrust reduction, and reduction in cooling flows) result in the reduction in TSEC for LH_2 Case 1 (of ~ 3-4%) and Case 3 (of 6-8%), compared to Jet-A engine, which can be observed from Tables 5, 6, and 7 (and Tables SI 34 [climb] and SI 35 [loiter] in SI §5.3).

Moreover, Figure 3 is useful to the reader for mapping out TSEC and thrust for both Jet-A and LH_2 cases at on-design and different off-design points in the flight mission. Future research could leverage this data to create an equation or surrogate model that estimates TSEC or TSFC based on the throttle setting for LH_2 engines. Such a model would be beneficial for multi-point design and optimization of LH_2 aircraft within the design space.

3.1.3 Effect on engine weight and dimensions

It can be seen from Table 5 that the engine weight decreases from Case 1 to Case 3 of LH_2. Jet-A and all three cases of LH_2 use the same stage counts of turbomachinery and advanced materials. The drop in engine weight is primarily attributable to the decreasing fan diameter (huge component in the engine) from Case 1 to Case 3 of LH_2 (see Table 5). In Case 2 and Case 3 of LH_2, as described before, the fan diameter is removed as a design constraint/target since Dincer [59], Verstraete [60], and Nojoumi [61] mention that for a LH_2 powered aircraft, the thrust requirement reduces and that the engine becomes smaller in size. In Case 2 and Case 3 of LH_2, this work is specifically trying to optimise the engine as per the thrust requirement of the aircraft and based on the suggestions of the above literature. Thus, the fan diameter is removed as a design constraint/target. Case 2 and Case 3 of LH_2 have the effect of lighter aircraft (lower thrust requirement, engine weight and fan size, and for Case 3 no cooling flows) for LH_2 use absorbed in them, compared to Jet-A and Case 1 of LH_2.

Figure 4 shows the cross-sectional view of the Jet-A powered engine overlapped with the three cases of LH_2 powered engine designed in this work (obtained from GasTurb 13). This figure also shows the diameter of the fan (a design requirement) and length of the engine. It can be observed from Figure 4 that LH_2 engine diameter and length reduce from Case 1 to Case 3.

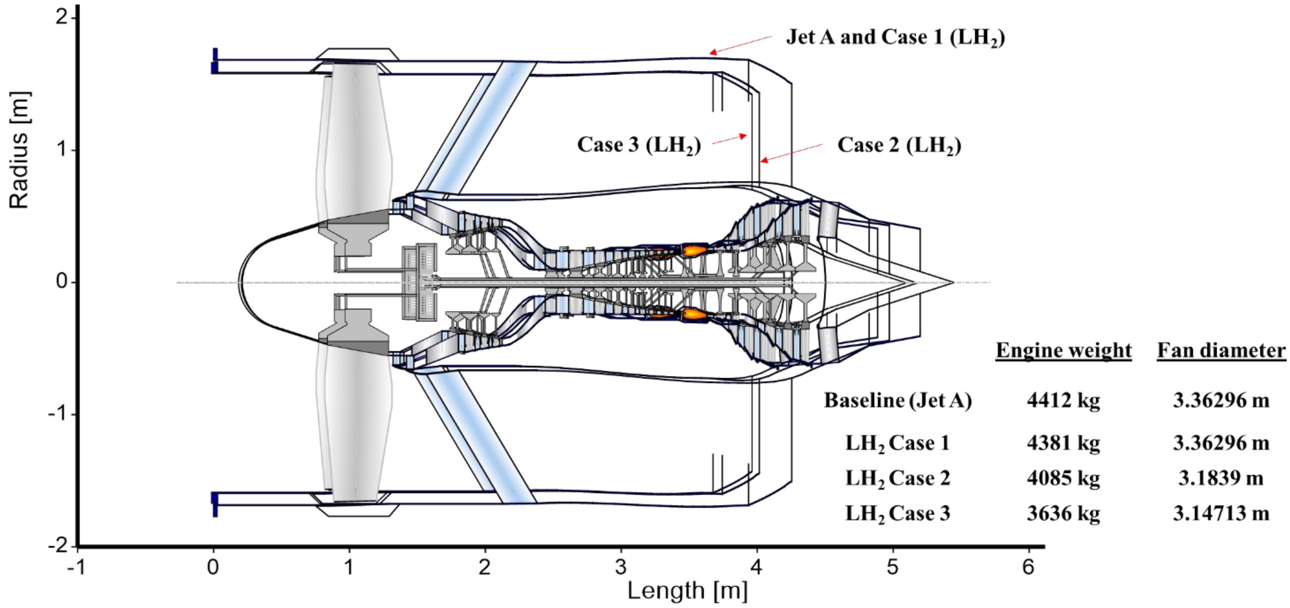

Figure 4. Cross-sectional view of the Jet-A (and 100% SPK) powered engine overlapped with the three cases of LH_2 powered engine designed in this work

Overall, it is observed that LH_2 engines are lighter, and colder (lower TET) than the baseline/Jet-A engine. Especially, the optimised LH_2 engines (Case 2 and Case 3) are smaller, shorter, colder, and lighter than Jet-A engine or LH_2 Case 1 engine. Additionally, LH_2 engines will have significantly improved engine and turbine life (discussed in §3.1.1), and resultantly cost savings. Lower engine weight implies fuel weight (cost and emissions) reduction during aircraft operation. Smaller engine size (diameter and length) implies more ground clearance, and it positively affects the aircraft operations and aircraft design in terms of wing, landing gear, and/or airframe design.

3.2 Evolution of engine technology

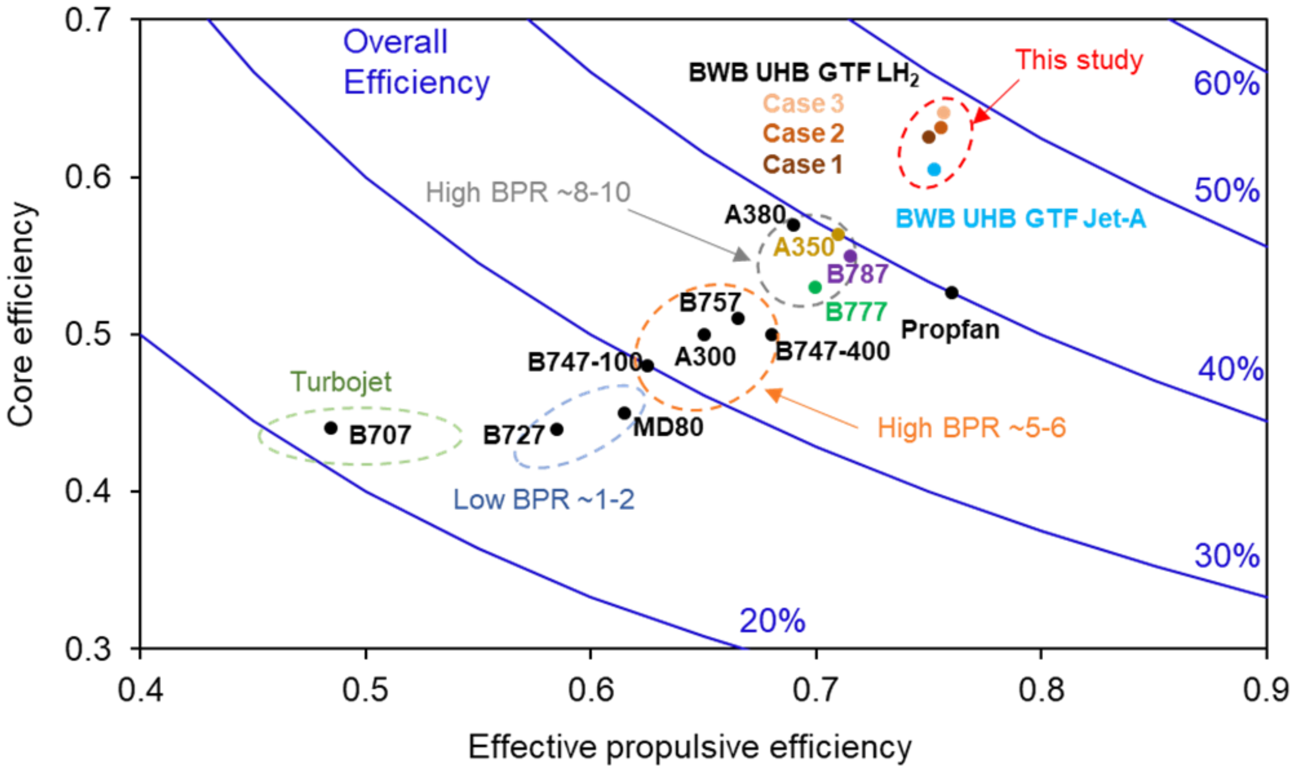

Figure 5. Cruise efficiencies of existing engines and engines modelled in this work (data source [100])

Figure 5 shows cruise efficiencies of existing engines and engines modelled in this work (data source [100]). The effective propulsive efficiency is the product of propulsive efficiency and transmission efficiency, and the core efficiency represents the engine thermal efficiency [100]. The overall efficiency is the product of the effective propulsive efficiency and core efficiency [100]. These efficiencies at cruise for all engines designed in this work are listed in Table 7. According to a study by Benzakein [101], UHB engines are expected to have overall efficiency in the range of 0.4 – 0.5 (depending on the BPR and OPR combinations). It can be observed from Figure 5 that the overall efficiencies of the UHB engines modelled in this work (UHB GTF powered by Jet-A, and three LH_2 cases) are similar to the expected values. The different efficiencies during cruise for all aircraft engines in Figure 5 are included in SI §5.4 in Table SI 36. Additionally, Figure 5 is useful to the reader for contextualising the findings of this work on future Jet-A and LH_2 UHB GTF engine in terms of evolution of turbofan engine technology.

Lastly, in Table 5 (TOC), Table 6 (SLS), Table 7 (cruise), Table SI 34 (climb) [SI §5.3], and Table SI 35 (loiter) [SI §5.3], the engine performance parameters (temperature, pressure, fuel-air ratio, and residence time) are known for both Jet-A and LH_2 at all points in mission. Additionally, Figure 5 (or Table SI 36 in SI §5.4) provides propulsive efficiency for both Jet-A and LH_2 during cruise. Similarly, for 100% SPK, all of the above engine performance parameters are provided in in SI §5.2. Using this data, emissions (like NO_x) and contrails modelling can be conducted for Jet-A, LH_2, and 100% SPK UHB GTF engine.

In a first, a comprehensive database of engine performance is provided that would enable future studies on engine and aircraft design, and aircraft emissions and contrails modelling, especially for LH_2 use.

3.3 Limitations of the present work

The estimation of the engine performance (TSFC, weight, thermodynamic properties, etc.) is conducted using GasTurb (zero-dimensional and/or one-dimensional analysis). Such level of analysis uses simplistic loss models for the performance analysis. In a high-fidelity analysis of engine performance, performance loss due to shock waves and air-foil geometry (used in turbomachinery) would also be accounted. These affect the engine performance and geometry (weight). Additionally, the engine performance during climb, cruise, and loiter, are considered to be average performance values during each of these flight segments. Moreover, LH_2 use requires modifications to fuel lines, and the installation of a heat exchanger to promote phase change of hydrogen from liquid to gas before it is injected into the combustor. The weights of the said heat exchanger and modified fuel lines are typically considered in the aircraft operating empty weight. Furthermore, hydrogen use in this work is limited for a fixed UHB GTF engine, and its use could be more efficient in variable geometry turbofan engines and/or distributed propulsion. Overall, the engine performance estimation in this work is a low fidelity analysis and errors in engine performance metrics are expected.

4. Conclusion

The potential of LH_2 aircraft to weigh less than those powered by Jet-A could lead to reduced engine thrust needs. This underscores the critical importance of considering the thermodynamic and energy performance of a hydrogen-powered aircraft engine, and its design and optimisation. In this work, using GasTurb 13 software, UHB GTF engines powered by Jet-A and LH_2 (separately) are designed by employing future materials and component efficiencies. The hydrogen powered gas turbine engine cycle is studied in detail. Three cases of LH_2 engines are considered and these are: same thrust production (unoptimized, Case 1), optimised for reduced thrust requirement (Case 2), and optimised for reduced thrust requirement but without turbine cooling flows (Case 3). The results comprise of performance analysis at on-design point and off-design points. Additionally, a simple 'major species' combustion model used in this work quantitatively explains the reasons behind the drop in hydrogen combustor temperature or increase in the specific heat of combustion products of hydrogen, for same thrust production, compared to Jet-A. There are three important effects of LH_2 on the engine TSFC relative to Jet-A: higher gravimetric energy density during combustion; higher specific heat of combustion products; and reduced aircraft thrust and weight. The first two effects are applicable to Case 1 LH_2 engine, and all three effects are applicable to case 2 and case 3 LH_2 engine. The TSEC for case 3 LH_2 engine is 6-8% lower than Jet-A. We observe that optimised LH_2 engines have 11% smaller diameter, 5.5 – 7.5% shorter length, 6 – 14% lower TET and 7 – 17% lower weight compared to Jet-A and unoptimised LH_2 engine. The results of this work will help future research on design of hydrogen engines and aircraft, and LH_2 aircraft emissions and contrails modelling.

Acknowledgments/Funding

The research conducted in this work is completely funded by the *President's PhD Scholarship* at *Imperial College London*. The authors are thankful to all donors who contribute to these funds and to *Imperial College London* for its support.

Declaration of competing interest

The authors declare that they have no known competing financial interests or personal relationships that could have appeared to influence the work reported in this paper.

References

[1] Boeing. COMMERCIAL MARKET OUTLOOK 2023–2042 2023. https://www.boeing.com/commercial/market/commercial-market-outlook/index.page (accessed February 10, 2024).

[2] Lee DS. The current state of scientific understanding of the non-CO2 effects of aviation on climate. Manchester Metrop Univ 2018. https://assets.publishing.service.gov.uk/government/uploads/system/uploads/attachment_data/file/813342/non-CO2-effects-report.pdf (accessed January 2, 2020).

[3] Lee DS, Fahey DW, Skowron A, Allen MR, Burkhardt U, Chen Q, et al. The contribution of global aviation to anthropogenic climate forcing for 2000 to 2018. Atmos Environ 2021;244:117834. https://doi.org/10.1016/J.ATMOSENV.2020.117834.

[4] Hupe J. Setting the Scene-Aviation and Climate Change. ICAO_Aviation_Green_Recovery_Seminar 2020. https://www.icao.int/Meetings/GreenRecoverySeminar/Documents/1.1 ICAO AGR - Setting the scene.pdf (accessed June 5, 2021).

[5] Khalifa R, Alherbawi M, Elomri A, Al-Ansari T. Alternative fuels' blending model to facilitate the implementation of carbon offsetting and reduction Scheme for International Aviation. Fuel 2022;326:124974. https://doi.org/10.1016/J.FUEL.2022.124974.

[6] Jagtap SS. Assessment of feedstocks for blended alcohol-to-jet fuel manufacturing from standalone and distributed scheme for sustainable aviation. AIAA Propuls. Energy 2019 Forum, Indianapolis, Indiana: American Institute of Aeronautics and Astronautics; 2019. https://doi.org/10.2514/6.2019-3887.

[7] Jagtap SS. Sustainability assessment of hydro-processed renewable jet fuel from algae from market-entry year 2020: Use in passenger aircrafts. 16th AIAA Aviat. Technol. Integr. Oper. Conf., Reston, Virginia: American Institute of Aeronautics and Astronautics; 2016. https://doi.org/10.2514/6.2016-4367.

[8] Jagtap SS. Evaluation of blended Fischer-Tropsch jet fuel feedstocks for minimizing human and environmental health impacts of aviation. AIAA Propuls. Energy 2019 Forum, Indianapolis, Indiana: American Institute of Aeronautics and Astronautics; 2019. https://doi.org/10.2514/6.2019-4412.

[9] Jagtap SS. Comparative assessment of manufacturing setups for blended sugar-to-aviation fuel production from non-food feedstocks for green aviation. AIAA Propuls. Energy 2019 Forum, Indianapolis, Indiana: American Institute of Aeronautics and Astronautics; 2019. https://doi.org/10.2514/6.2019-4332.

[10] Jagtap SS, Childs PRN, Stettler MEJ. Energy performance evaluation of alternative energy vectors for subsonic long-range tube-wing aircraft. Transp Res Part D Transp Environ 2023;115:103588. https://doi.org/10.1016/J.TRD.2022.103588.

[11] World Economic Forum. Target True Zero Unlocking Sustainable Battery and Hydrogen-Powered Flight - Insight Report. 2022.

[12] Jagtap SS, Childs PRN, Stettler MEJ. Performance sensitivity of subsonic liquid

hydrogen long-range tube-wing aircraft to technology developments. Int J Hydrogen Energy 2024;50:820–33. https://doi.org/10.1016/J.IJHYDENE.2023.07.297.

[13] Tiwari S, Pekris MJ, Doherty JJ. A review of liquid hydrogen aircraft and propulsion technologies. Int J Hydrogen Energy 2024;57:1174–96. https://doi.org/10.1016/J.IJHYDENE.2023.12.263.

[14] Dietl T, Karger J, Kaupe K, Pfemeter A, Weber P, Zakrzewski A, et al. POLARIS-DESIGN OF A LIQUID HYDROGEN TURBO-ELECTRIC TRANSPORT AIRCRAFT, Deutsche Gesellschaft für Luft- und Raumfahrt; 2018. https://doi.org/10.25967/480344.

[15] Druot TYJ, Peteilh N, Roches P, Monrolin N. Hydrogen Powered Airplanes, an exploration of possible architectures leveraging boundary layer ingestion and hybridization. AIAA Sci Technol Forum Expo AIAA SciTech Forum 2022 2022. https://doi.org/10.2514/6.2022-1025.

[16] Ashcraft SW, Padron AS, Pascioni KA, Stout GW, Huff DL. Review of propulsion technologies for N+3 subsonic vehicle concepts (Report # 20110022435) 2011. https://ntrs.nasa.gov/citations/20110022435.

[17] DLR. Conceptual study for environment-friendly flight. DLR 2020. https://www.dlr.de/en/latest/news/2020/02/20200504_conceptual-study-for-environment-friendly-flight (accessed May 26, 2021).

[18] Delgado Gosálvez M, Ham van J, Joosten S, Juschus D, Nieuwerth G, Pelt van T, et al. Green Flying: Final Report. TU Delft 2018. https://www.researchgate.net/publication/326294480_The_Greenliner_Green_Flying_Final_Report_DSE_Group_8 (accessed January 2, 2020).

[19] Abu Kasim AFB, Chan MSC, Marek EJ. Performance and failure analysis of a retrofitted Cessna aircraft with a Fuel Cell Power System fuelled with liquid hydrogen. J Power Sources 2022;521:230987. https://doi.org/10.1016/J.JPOWSOUR.2022.230987.

[20] Job S, Campbell M, Hall B, Hamadache Z, Kumar N. SUSTAINABILITY REPORT - The Lifecycle Impact of Hydrogen-Powered Aircraft. 2022.

[21] Nicolay S, Karpuk S, Liu Y, Elham A. Conceptual design and optimization of a general aviation aircraft with fuel cells and hydrogen. Int J Hydrogen Energy 2021;46:32676–94. https://doi.org/10.1016/J.IJHYDENE.2021.07.127.

[22] Thoennes M, Busse A, Eckstein L. Forecast of Performance Parameters of Automotive Fuel Cell Systems - Delphi Study Results. Fuel Cells 2014;14:781–91. https://doi.org/10.1002/fuce.201400035.

[23] Waddington EG, Merret JM, Ansell PJ. Impact of LH2 Fuel Cell-Electric Propulsion on Aircraft Configuration and Integration. AIAA Aviat Aeronaut Forum Expo AIAA Aviat Forum 2021 2021. https://doi.org/10.2514/6.2021-2409.

[24] Vonhoff G. Conceptual Design of Hydrogen Fuel Cell Aircraft: Flying on hydrogen for a more sustainable future. Delft University of Technology, 2021.

[25] Nicolosi F, Marciello V, Orefice F. Conceptual Design of a Hydrogen-Propelled Aircraft with Distributed Electric Propulsion 2022. https://doi.org/10.2514/6.2022-3205.

[26] Pastra CL, Cinar G, Mavris DN. Feasibility and benefit assessments of hybrid hydrogen fuel cell and battery configurations on a regional turboprop aircraft 2022. https://doi.org/10.2514/6.2022-3290.

[27] Brelje BJ, Martins JRRA. Aerostructural wing optimization for a hydrogen fuel cell aircraft. AIAA Scitech 2021 Forum 2021:1–18. https://doi.org/10.2514/6.2021-1132.

[28] Svensson F. Potential of reducng the environmental impact of civil subsonic aviation by using liquid hydrogen. Cranfield University, 2005.

[29] Prewitz M, Bardenhagen A, Beck R. Hydrogen as the fuel of the future in aircrafts – Challenges and opportunities. Int J Hydrogen Energy 2020;45:25378–85. https://doi.org/10.1016/J.IJHYDENE.2020.06.238.

[30] Silberhorn D, Atanasov G, Walther J-N, Zill T. ASSESSMENT OF HYDROGEN FUEL TANK INTEGRATION AT AIRCRAFT LEVEL. Inst Transp Res 2019.

[31] Yang B, Mane M, Crossley WA. An Approach to Evaluate Fleet Level CO2 Impact of Introducing Liquid-Hydrogen Aircraft to a World-Wide Network 2022. https://doi.org/10.2514/6.2022-3313.

[32] Onorato G, Proesmans P, Hoogreef MFM. Assessment of hydrogen transport aircraft: Effects of fuel tank integration. CEAS Aeronaut J 2022;1:1–33. https://doi.org/10.1007/S13272-022-00601-6/TABLES/11.

[33] Hoelzen J, Silberhorn D, Zill T, Bensmann B, Hanke-Rauschenbach R. Hydrogen-powered aviation and its reliance on green hydrogen infrastructure – Review and research gaps. Int J Hydrogen Energy 2022;47:3108–30. https://doi.org/10.1016/J.IJHYDENE.2021.10.239.

[34] Lammen WF, Peerlings B, Sman ES van der, Kos J. Hydrogen-powered propulsion aircraft: conceptual sizing and fleet level impact analysis. Netherlands Aerosp Cent NLR 2022. http://hdl.handle.net/10921/1587 (accessed October 7, 2022).

[35] Silberhorn D, Dahlmann K, Görtz A, Linke F, Zanger J, Rauch B, et al. Climate Impact Reduction Potentials of Synthetic Kerosene and Green Hydrogen Powered Mid-Range Aircraft Concepts. Appl Sci 2022, Vol 12, Page 5950 2022;12:5950. https://doi.org/10.3390/APP12125950.

[36] Massaro MC, Biga R, Kolisnichenko A, Marocco P, Monteverde AHA, Santarelli M. Potential and technical challenges of on-board hydrogen storage technologies coupled with fuel cell systems for aircraft electrification. J Power Sources 2023;555:232397. https://doi.org/10.1016/J.JPOWSOUR.2022.232397.

[37] Mouvand S, Noharet Q. Preliminary design and simulation of a hydrogen-powered regional aircraft. AIAA Aviat 2023 Forum 2023. https://doi.org/10.2514/6.2023-4546.

[38] Kolisnichenko A, Biga R, Di Fede F. Evaluation of Technology Gravimetric Index Targets for Zero Emissions Regional Flight. AIAA Aviat 2023 Forum 2023. https://doi.org/10.2514/6.2023-4540.

[39] Jagtap SS. Systems evaluation of subsonic hybrid-electric propulsion concepts for NASA N+3 goals and conceptual aircraft sizing. Int J Automot Mech Eng 2019;16:7259–7286. https://doi.org/https://doi.org/10.15282/ijame.16.4.2019.07.0541.

[40] Seyam S, Dincer I, Agelin-Chaab M. Economic and environmental impact assessments

of hybridized aircraft engines with hydrogen and other fuels. Int J Hydrogen Energy 2022;47:11669–85. https://doi.org/10.1016/J.IJHYDENE.2022.01.171.

[41] Svensson C, Oliveira AAM, Grönstedt T. Hydrogen fuel cell aircraft for the Nordic market. Int J Hydrogen Energy 2024;61:650–63. https://doi.org/10.1016/J.IJHYDENE.2024.02.382.

[42] Jagtap SS. An Apparatus for Exchanging Heat with Flow in an Annulus. J Eng Sci Technol Rev 2017;10:173–6.

[43] Jagtap SS. Heat recuperation system for the family of shaft powered aircraft gas turbine engines, 2016.

[44] Gomez A, Smith H. Liquid hydrogen fuel tanks for commercial aviation: Structural sizing and stress analysis. Aerosp Sci Technol 2019;95:105438. https://doi.org/10.1016/j.ast.2019.105438.

[45] Cipolla V, Zanetti D, Salem KA, Binante V, Palaia G. A Parametric Approach for Conceptual Integration and Performance Studies of Liquid Hydrogen Short–Medium Range Aircraft. Appl Sci 2022, Vol 12, Page 6857 2022;12:6857. https://doi.org/10.3390/APP12146857.

[46] Troeltsch F, Engelmann M, Peter F, Kaiser J, Hornung M, Scholz AE. Hydrogen powered long haul aircraft with minimized climate impact. AIAA Aviat 2020 FORUM 2020:14. https://doi.org/10.2514/6.2020-2660.

[47] Proesmans P-J, Vos R. Comparison of Future Aviation Fuels to Minimize the Climate Impact of Commercial Aircraft 2022. https://doi.org/10.2514/6.2022-3288.

[48] Verstraete D, Hendrick P, Pilidis P, Ramsden K. Hydrogen fuel tanks for subsonic transport aircraft. Int J Hydrogen Energy 2010;35:11085–98. https://doi.org/10.1016/j.ijhydene.2010.06.060.

[49] Verstraete D. On the energy efficiency of hydrogen-fuelled transport aircraft. Int J Hydrogen Energy 2015;40:7388–94. https://doi.org/10.1016/j.ijhydene.2015.04.055.

[50] Brewer GD. Hydrogen aircraft technology. CRC Press; 2017. https://doi.org/10.1201/9780203751480.

[51] Reinhard Faass. CRYOPLANE 2001:6. https://www.fzt.haw-hamburg.de/pers/Scholz/dglr/hh/text_2001_12_06_Cryoplane.pdf (accessed December 28, 2019).

[52] CleanSky2-FCH. Hydrogen-powered aviation. CleanSky2 - Fuel Cell Hydrog 2020. https://doi.org/10.2843/766989.

[53] Air-Liquide. Hydrogen storage on board aeronef and ground infrastructure : Air Liquide Advanced Technologies-Workshop on aeronautical applications of fuel cell and hydrogen technologies. FCH - CleanSky Jt Work 2015.

[54] Huete J, Nalianda D, Pilidis P. Impact of tank gravimetric efficiency on propulsion system integration for a first-generation hydrogen civil airliner. Aeronaut J 2022;126:1324–32. https://doi.org/10.1017/AER.2022.60.

[55] Huete J, Nalianda D, Pilidis P. Propulsion system integration for a first-generation hydrogen civil airliner? Aeronaut J 2021;125:1654–65.

https://doi.org/10.1017/AER.2021.36.

[56] Grewe V, Bock L, Burkhardt U, Dahlmann K, Gierens K, Hüttenhofer L, et al. Assessing the climate impact of the AHEAD multi-fuel blended wing body. Meteorol Zeitschrift 2017;26:711–25. https://doi.org/10.1127/METZ/2016/0758.

[57] Adler EJ, Martins JRRA. Blended Wing Body Configuration for Hydrogen-Powered Aviation. Https://DoiOrg/102514/1C037582 2024:1–15. https://doi.org/10.2514/1.C037582.

[58] de Nercy - Maingard H, Palies P. Impact of Fuel Type on Aircraft Range: An Initial Optimization Study 2023. https://doi.org/10.1115/GT2023-103247.

[59] Dincer I, Acar C. A review on potential use of hydrogen in aviation applications. Int J Sustain Aviat 2016;2:74. https://doi.org/10.1504/IJSA.2016.076077.

[60] Verstraete D. The Potential of Liquid Hydrogen for long range aircraft propulsion. Cranfield University; 2009.

[61] Nojoumi H, Dincer I, Naterer GF. Greenhouse gas emissions assessment of hydrogen and kerosene-fueled aircraft propulsion. Int J Hydrogen Energy 2009;34:1363–9. https://doi.org/10.1016/J.IJHYDENE.2008.11.017.

[62] Prater R. Methods for Decarbonized Aeroengine Combustor Design. University of Tennessee, 2023.

[63] Marek C, Smith T, Kundu K. Low Emission Hydrogen Combustors for Gas Turbines Using Lean Direct Injection. 41st AIAA/ASME/SAE/ASEE Jt. Propuls. Conf. Exhib., Reston, Virigina: American Institute of Aeronautics and Astronautics; 2005. https://doi.org/10.2514/6.2005-3776.

[64] Bijewitz J, Seitz A, Hornung M. Architectural Comparison of Advanced Ultra-High Bypass Ratio Turbofans for Medium to Long Range Application. Dtsch. Luft- und Raumfahrtkongress 2014, 2014.

[65] Kestner BK, Schutte JS, Gladin JC, Mavris DN. Ultra high bypass ratio engine sizing and cycle selection study for a subsonic commercial aircraft in the N+2 timeframe. Proc. ASME Turbo Expo, vol. 1, 2011, p. 127–37. https://doi.org/10.1115/GT2011-45370.

[66] Corchero G, Montañ JL. An approach to the use of hydrogen for commercial aircraft engines. Proc Inst Mech Eng Part G J Aerosp Eng 2005;219:35–44. https://doi.org/10.1243/095441005X9139.

[67] Beck R, Bieler J, Borsutzki S, Cabac Y, Dehmel J, Khosravi R, et al. Efficiency meets sky. Jt NASA/DLR Aeronaut Des Chall 2017-18 2018. https://www.dlr.de/dlr/Portaldata/1/Resources/documents/2018/TU_Berlin_EFFICIENCY_MEETS_SKY.pdf (accessed January 19, 2020).

[68] Atma PN, Lamkin AH, Martins JR. Comparing Hydrogen and Jet-A for a Ultra High-Bypass Turbofan with Water Recirculation. 2023. https://doi.org/10.2514/6.2023-4018.

[69] Osigwe EO, Gad-Briggs A, Nikolaidis T, Jafari S, Sethi B, Pilidis P. Thermodynamic Performance and Creep Life Assessment Comparing Hydrogen- and Jet-Fueled Turbofan Aero Engine. Appl Sci 2021, Vol 11, Page 3873 2021;11:3873.

https://doi.org/10.3390/APP11093873.

[70] Carter RE, Agarwal RK. Development of a Liquid Hydrogen Combustion High Bypass Geared Turbofan Model in NPSS 2022. https://doi.org/10.2514/6.2022-3431.

[71] Görtz A, Silberhorn D. THERMODYNAMIC POTENTIAL OF TURBOFAN ENGINES WITH DIRECT COMBUSTION OF HYDROGEN. Proceedings_of_the_33rd_Congress_of_the_International_ Counc 2022.

[72] Balli O, Ozbek E, Ekici S, Midilli A, Hikmet Karakoc T. Thermodynamic comparison of TF33 turbofan engine fueled by hydrogen in benchmark with kerosene. Fuel 2021;306:121686. https://doi.org/10.1016/J.FUEL.2021.121686.

[73] Greitzer EM, Bonnefoy PA, De la Rosa Blanco E, Dorbian CS, Drela M, Hall DK, et al. N+3 Aircraft Concept Designs and Trade Studies, Final Report, Volume 1. 2010.

[74] Nickol CL, Haller WJ. Assessment of the Performance Potential of Advanced Subsonic Transport Concepts for NASA's Environmentally Responsible Aviation Project. 54th AIAA Aerosp. Sci. Meet., Reston, Virginia: American Institute of Aeronautics and Astronautics; 2016. https://doi.org/10.2514/6.2016-1030.

[75] Marszalek N. PRELIMINARY ANALYSIS OF THERMODYNAMIC CYCLE OF TURBOFAN ENGINE FUELLED BY HYDROGEN. J KONES Powertrain Transp 2018;25. https://doi.org/10.5604/01.3001.0012.4351.

[76] Derakhshandeh P, Ahmadi A, Dashti R. Simulation and technical-economic-environmental optimization of the General Electric GE90 hydrogen turbofan engine. Int J Hydrogen Energy 2021;46:3303–18. https://doi.org/10.1016/J.IJHYDENE.2020.10.182.

[77] Oğur E, Koç A, Yağlı H, Koç Y, Köse Ö. Thermodynamic, economic, and environmental analysis of a hydrogen-powered turbofan engine at varying altitudes. Int J Hydrogen Energy 2024;55:1203–16. https://doi.org/10.1016/J.IJHYDENE.2023.11.252.

[78] Palies PP. Hydrogen Thermal-Powered Aircraft Combustion and Propulsion System. J Eng Gas Turbines Power 2022;144. https://doi.org/10.1115/1.4055270/1145558.

[79] Boggia S, Jackson A. Some Unconventional Aero Gas Turbines Using Hydrogen Fuel. Am Soc Mech Eng Int Gas Turbine Institute, Turbo Expo IGTI 2009;2 B:683–90. https://doi.org/10.1115/GT2002-30412.

[80] Jackson AJB. Optimisation of aero and industrial gas turbine design for the environment 2009.

[81] Verstraete D. Long range transport aircraft using hydrogen fuel. Int J Hydrogen Energy 2013;38:14824–31. https://doi.org/10.1016/j.ijhydene.2013.09.021.

[82] GasTurb - GasTurb n.d. https://gasturb.de/software/gasturb.html (accessed April 10, 2020).

[83] SwRI. Numerical Propulsion System Simulation (NPSS) n.d. https://www.swri.org/consortia/numerical-propulsion-system-simulation-npss (accessed September 14, 2023).

[84] DLR - Institute of Propulsion Technology -. GTlab n.d.

https://www.dlr.de/at/en/desktopdefault.aspx/tabid-9029/ (accessed October 7, 2023).

[85] Quinlan JR, Gern FH. Conceptual design and structural optimization of nasa environmentally responsible aviation (ERA) hybrid wing body aircraft. 57th AIAA/ASCE/AHS/ASC Struct. Struct. Dyn. Mater. Conf., American Institute of Aeronautics and Astronautics; 2016. https://doi.org/10.2514/6.2016-0229.

[86] Nickol CL. Hybrid wing body configuration scaling study. 50th AIAA Aerosp. Sci. Meet. Incl. New Horizons Forum Aerosp. Expo., Nashville, Tennessee: 2012. https://doi.org/10.2514/6.2012-337.

[87] Thomas RH, Burley CL, Nickol CL. Assessment of the Noise Reduction Potential of Advanced Subsonic Transport Concepts for NASA's Environmentally Responsible Aviation Project. 54th AIAA Aerosp. Sci. Meet., Reston, Virginia: American Institute of Aeronautics and Astronautics; 2016. https://doi.org/10.2514/6.2016-0863.

[88] Kurzke J. GasTurb 13. GasTurb GmbH 2017. https://gasturb.de/software/gasturb.html.

[89] Hendricks ES. A multi-level multi-design point approach for gas turbine cycle and turbine conceptual design. Georgia Institute of Technology, 2017.

[90] Walsh PP, Fletcher P. Gas Turbine Performance. Wiley; 2004. https://doi.org/10.1002/9780470774533.

[91] Pratt and Whitney PW1100G Geared Turbofan Engine | The Flying Engineer n.d. http://theflyingengineer.com/flightdeck/pw1100g-gtf/ (accessed December 6, 2019).

[92] Halliwell I. An Ultra-High Bypass Ratio Turbofan Engine for the Future 2014. https://pdfslide.us/documents/undergraduate-team-engine-student-design-competition-2014-undergraduate.html (accessed December 9, 2019).

[93] Dicarlo JA. Advances in SiC/SiC Composites for Aero-Propulsion. 2013.

[94] Bansal RK. A Textbook of Strength of Materials. Laxmi Publications; 2010.

[95] Halliwell I. An Improved Engine for a High Altitude Long Endurance Unmanned Air Vehicle. AIAA, ASME IGTI 2012. https://files.asme.org/igti/33208.pdf (accessed December 8, 2019).

[96] Jagtap SS, Childs PRN, Stettler MEJ. Conceptual design-optimisation of a subsonic hydrogen-powered long-range blended-wing-body aircraft (in review). Int J Hydrogen Energy ~~2024~~2025.

[97] Kirby MR. A methodology for technology identification, evaluation, and selection in conceptual and preliminary aircraft design. Georgia Institute of Technology, 2001.

[98] Kundu AK, Price MA, Riordan D. Conceptual Aircraft Design : an Industrial Perspective. First. John Wiley & Sons, Incorporated; 2019.

[99] Airbus. Liquid Hydrogen Fuelled Aircraft-System Analysis: CRYOPLANE Final Technical report 2003. https://www.fzt.haw-hamburg.de/pers/Scholz/dglr/hh/text_2004_02_26_Cryoplane.pdf (accessed December 30, 2019).

[100] National-Academies-of-Sciences-Engineering-and-Medicine. Commercial Aircraft Propulsion and Energy Systems Research. Washington, D.C.: National Academies Press; 2016. https://doi.org/10.17226/23490.

[101] Benzakein MJ. What does the future bring? A look at technologies for commercial aircraft in the years 2035–2050. Propulsion_and_Power Res 2014;3:165–74. https://doi.org/10.1016/J.JPPR.2014.11.004.